

CHAPTER FOUR

One-Dimensional Energy Eigenvalue Problems

Among eigenvalue problems, the problem of finding the eigenfunctions and eigenvalues of the energy operator (the Hamiltonian) plays a special role. The total energy of a system is a constant, and is thus an important characteristic. Another reason is that the energy levels (i.e., energy eigenvalues) of a system often determine properties such as chemical bonding, crystal structure, electrical and optical properties, and rates of chemical reactions. The nature of the energy levels thus has a direct bearing on the way we perceive materials (color, as an example) and utilize them.

In this chapter we consider some simple one-electron, one-dimensional energy eigenvalue problems. In each case we solve the time-independent Schrödinger equation

$$\left(\frac{\hat{p}^2}{2m} + V(x)\right)u_E(x) = E u_E(x) \quad (4.1)$$

where the energy operator (Hamiltonian) $\hat{p}^2/2m + V(x)$ is the sum of the kinetic and potential energies of a particle. The solution yields the energy eigenvalues E and the eigenfunctions $u_E(x)$. $V(x)$ is the potential energy function.

4.1 INFINITE POTENTIAL WELL

Consider a particle of mass m moving in a potential one-dimensional well that is zero over the interval $-a < x < a$ and infinite elsewhere, as shown in Fig.

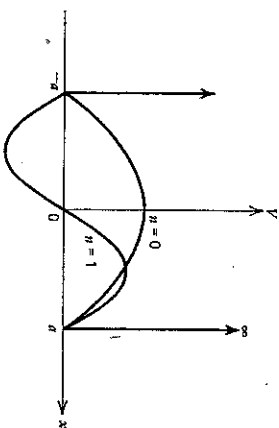


Figure 4.1 The infinite potential well and the first two ($n=0, 1$) eigenfunctions of the bound particle.

4.1. The energy eigenvalue equation is given in (4.1), where, following (3.20), we set $\hat{p} \rightarrow -\hbar \partial/\partial x$. The result is

$$\left(-\frac{\hbar^2}{2m} \frac{\partial^2}{\partial x^2} + V(x)\right)u_E(x) = E u_E(x) \quad (4.2)$$

The solution in the region $-a < x < a$, where $V(x)=0$, is of the form

$$u_E = \cos kx \quad \text{or} \quad u_E = \sin kx \quad (4.3)$$

where

$$k = \sqrt{2mE/\hbar^2} \quad (4.4)$$

Outside the region $-a < x < a$, $u_E(x)$ must be zero. This follows from (4.2), since the potential $V(x)$ is infinite. In order that $u_E(x)$ vanish at $x = \pm a$, we must choose

$$k = (2n+1) \frac{\pi}{2a} \quad (n=0, 1, 2, 3, \dots) \quad (4.5)$$

in the case of the even (cosine) solution, and

$$k = 2n \left(\frac{\pi}{2a}\right) \quad (n=1, 2, 3) \quad (4.6)$$

for the odd (sine) functions.

The even and odd solutions thus assume, respectively, the form

$$u_E(x) = \frac{1}{\sqrt{2a}} \cos \left[\left(n + \frac{1}{2}\right) \frac{\pi x}{a} \right] \quad (4.7)$$

$$u_E(x) = \frac{1}{\sqrt{2a}} \sin \left(n \frac{\pi x}{a} \right) \quad (4.8)$$

where the normalization factor $(2a)^{-1/2}$ was added so that $\int_{-a}^a u_E^2(x) dx = 1$.

The energy expression

$$E = \frac{\hbar^2 k^2}{2m} \quad (4.9)$$

becomes, combining (4.5) and (4.6),

$$E_l = l^2 \frac{\pi^2 \hbar^2}{8ma^2} \quad (l=1, 2, 3, \dots) \quad (4.10)$$

The odd values of l belong to even solutions and vice versa. The lowest energy is associated with the even solution (cosine) with $n=0$ (or $l=1$). The next highest energy is that of the odd solution with $n=1$ ($l=2$). It follows from (4.5) and (4.6) that the solutions alternate between those of odd and even symmetry as the energy increases.

4.2 FINITE POTENTIAL WELL

Next consider the motion of an electron in a potential well with finite barriers of height V , as shown in Fig. 4.2. Since the potential well is symmetric [$V(x)=V(-x)$], the solutions of the Schrödinger equation

$$\left(-\frac{\hbar^2}{2m} \frac{d^2}{dx^2} + V(x) \right) u_E(x) = E u_E(x) \quad (4.11)$$

must possess odd symmetry [$u_E(-x) = -u_E(x)$] or even symmetry¹ [$u_E(x) = u_E(-x)$]. It is convenient to consider two different cases.

Case 1: $E < V$

In the internal region $|x| \leq a$ the solution of (4.11) is of the form

$$u_E(x) = \cos k_0 x, \sin k_0 x \quad (4.12)$$

$$k_0 = \sqrt{2mE}/\hbar \quad (4.13)$$

The solution for $x > a$ is of the form²

$$u_E(x) = C e^{-\kappa|x|} \quad (|x| > a) \quad (4.14)$$

$$\kappa = \sqrt{2m(V-E)}/\hbar \quad (4.15)$$

The alternate solution $\exp(\kappa x)$ has been eliminated on physical grounds, since $\int |u_E(x)|^2 dx$ must be finite. Since $V(x)$, and with it $u_E^2(x)$, are finite everywhere, $u_E^2(x)$ and $u_E(x)$ must be continuous everywhere including $x = \pm a$. We apply the continuity condition to the *even* solution and its derivative at

¹The relation between the symmetry of the eigenfunction and that of $V(x)$ is discussed more fully in Chapter 5.

²The solution for $x < -a$ can be obtained directly from the symmetry condition.

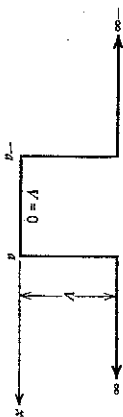


Figure 4.2 The finite potential well.

$x = a$ obtaining

$$\cos k_0 a = C e^{-\kappa a} \quad (4.16)$$

and

$$-k_0 \sin k_0 a = -\kappa C e^{-\kappa a}$$

so that

$$k_0 a \tan k_0 a = \kappa a \quad (4.17a)$$

Applying the boundary conditions to the odd solutions results in

$$k_0 a \cot k_0 a = -\kappa a \quad (4.17b)$$

In either case, the constants k_0 and κ must satisfy (4.17) while simultaneously being related through (4.13) and (4.15). The last two mentioned equations can be combined as

$$\kappa^2 a^2 + k_0^2 a^2 = \frac{2mV}{\hbar^2} a^2 \quad (4.18)$$

which is the equation of a circle in the κa , $k_0 a$ plane with a radius $\sqrt{2mVa^2}/\hbar^2$. We thus need to solve (4.17) and (4.18) for k_0 and κ . A graphical procedure for obtaining k_0 and κ is shown in Fig. 4.3.

The solutions correspond to the intersections in the upper half-plane ($\kappa > 0$) of the circle (4.18) with a plot of (4.17a). The first three solutions are designated as $n = 0, 2, 4$. We refer to the corresponding eigenstates as u_0, u_2, u_4 .

The constants κ and k_0 of the odd solutions are obtained in a similar manner as the coordinates of the intersections of the circle (4.18) with a plot of (4.17b). These are designated as $n = 1, 3, \dots$. The corresponding eigenstates are u_1, u_3, \dots .

It is evident from the graphical construction of Fig. 4.3 that the number of bound states—that is, the number of intersections—increases with V . If the value of V is such that

$$\frac{\pi}{2} < \sqrt{\frac{2mVa^2}{\hbar^2}} < (s+1)\frac{\pi}{2} \quad (4.19)$$

there exist exactly $s+1$ bound states. The state index n is thus equal to the number of zero crossings of $u_n(x)$. The first three eigenfunctions $n = 0, 1, 2$ are shown in Fig. 4.4. We note from Fig. 4.3 that the higher the state index n , the

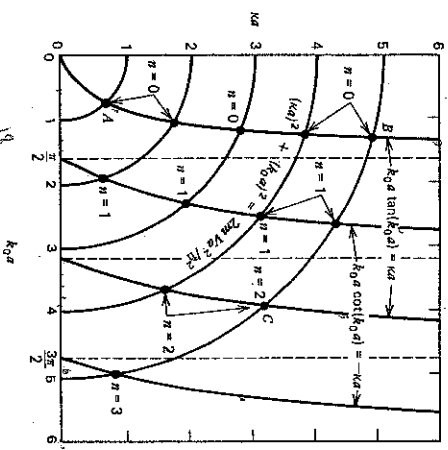


Figure 4.3 The graphical solution for obtaining the k and k_0 of the eigenfunction of a particle in a one-dimensional rectangular potential well. These are determined by the intersections (black dots) of the plots of (4.17a) (for even modes) and (4.17b) (for odd modes) with the circles (4.18). The radius of the circles is $\sqrt{2mV} a / h$. (A given problem involves only one circle)

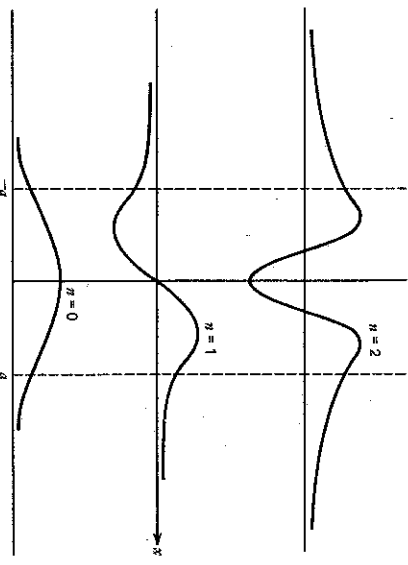


Figure 4.4 The first three bound states of a particle in a finite potential well.

smaller the value of k , hence the deeper the penetration of the corresponding $u_n(x)$ into the $|x| > a$ region.

The energy of the eigenstate $u_n(x)$ is, according to (4.13),

$$E_n = \frac{\hbar^2 k_n^2}{2m}$$

where k_{0n} is the value of k_0 of the mode u_n .

The solutions discussed in this section were all subject to the constraint $E < V$. Classical particles with energies $E < V$ cannot penetrate beyond the barrier to $|x| > a$. Yet in quantum mechanics we find that the probability distribution $|u_n(x)|^2$ is finite even for $|x| > a$. The quantum mechanical particle rushes in where its classical counterpart fears to tread.

Case 2: $E > V$

In this regime the particle energy exceeds that of the barrier and $k = \sqrt{2m(V-E)}/\hbar$ is imaginary so that the solution for (4.12)–(4.14) for $u_E(x)$ is sinusoidal everywhere. Consequently, the probability density is distributed over all space and the particle is *not bound*. Here it makes physical sense to consider the case of a particle approaching the well from one direction, and to inquire about the probability of either its passing across the barrier or its reflection from it. This subject is considered in the next section.

4.3 FINITE POTENTIAL BARRIER

Here we consider a particle incident from the left on a barrier of height V and width a , as shown in Fig. 4.5a. Our results will also apply to the potential well of Fig. 4.2 by replacing V with $-V$. We first consider the case when $E < V$, so that classically the particle would be turned back at $x=0$. The solution of the Schrödinger equation (4.2) is satisfied by taking

$$u_E(x) = \begin{cases} A e^{ikx} + A e^{-ikx} & (x < 0) \\ B e^{-kx} + C e^{kx} & (0 < x < a) \\ D e^{ik(x-a)} & (x > a) \end{cases} \quad (4.20)$$

$$k = \sqrt{2mE}/\hbar, \quad \kappa = \sqrt{2m(V-E)}/\hbar \quad (4.21)$$

In (4.20) we take the incident wave as $A e^{ikx}$ with a unit amplitude. The wave $A e^{-ikx}$ corresponds to a reflected wave (its momentum eigenvalue $-\hbar k$ is negative). At $x > a$, $u_E(x)$ is in the form of a particle wave traveling to the right. The form of $|u_E(x)|^2$ for $E < V$ is sketched in Fig. 4.5b. By imposing the continuity condition on $u_E(x)$ and $u'_E(x)$ at the boundaries $x=0$, $x=a$, we obtain four linear equations with the unknown coefficients A, B, C, D . Their solution is

$$D = \frac{2i\kappa k}{2i\kappa k \cosh \kappa a + (k^2 - \kappa^2) \sinh \kappa a} \quad (4.22)$$

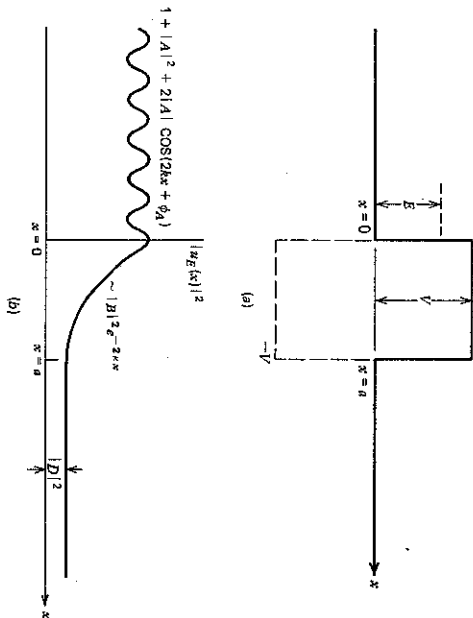


Figure 4.5 (a) The potential profile $V(x)$. (b) A plot of a typical probability distribution $|\psi_E(x)|^2$ for $E < V$. The plot inside the well, $0 < x < a$, is for the case $ka \gg 1$, where it approaches an exponential decay $|\psi_E(x)|^2 \propto \exp(-2kx)$.

The tunneling probability, that is, the probability that an incident particle penetrates beyond the barrier ($x > a$), is given by $|D|^2$.

$$T(E < V) \equiv |D|^2 = \frac{\sinh^2 \left(\sqrt{\frac{2m(V-E)}{\hbar^2}} \frac{a}{a} \right)}{1 + \frac{\sinh^2 \left(\sqrt{\frac{2m(V-E)}{\hbar^2}} \frac{a}{a} \right)}{4(E/V)(1-E/V)}} \quad (4.23)$$

We note that when $E < V$ the transmissivity $T(E)$ is always less than unity. When the incident particle energy exceeds that of the barrier ($E > V$), the constant k becomes imaginary, and instead of (4.23) we have

$$T(E > V) = \frac{\sin^2 \left(\sqrt{\frac{2m(E-V)}{\hbar^2}} \frac{a}{a} \right)}{1 + \frac{\sin^2 \left(\sqrt{\frac{2m(E-V)}{\hbar^2}} \frac{a}{a} \right)}{4(E/V)(E/V-1)}} \quad (4.24)$$

The behavior of $T(E)$ for both regimes, $E < V$ and $E > V$, is sketched in Fig. 4.6. Also plotted is the reflectivity $R = |A|^2$. It will be left as an exercise to show that

$$R + T = 1 \quad (4.25)$$

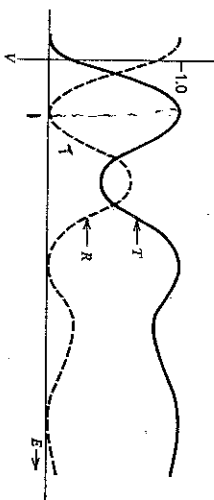


Figure 4.6 Transmission and reflection coefficients of a rectangular potential barrier.

Two important features of (4.23) and (4.24) stand out: (1) When the incident particle energy $E < V$, a region where classically the particle is turned back at $x=0$, there still exists a finite probability for penetrating—tunneling—through the barrier. This probability is given by (4.23). In the limit of small tunneling probability, $[2m(V-E)]^{1/2}(a/\hbar) \gg 1$, we may approximate (4.23) by

$$T(E) \approx 4 \left(\frac{E}{V} \right) \left(1 - \frac{E}{V} \right) \exp \left[-\sqrt{\frac{8m(V-E)}{\hbar^2}} \frac{a}{a} \right] \quad (4.26)$$

(2) At $E > V$ the transmission $T(E)$ goes through a series of unity maxima. Two such neighboring peaks, say E_2 and E_1 in Fig. 4.6, are characterized by having the electronic round trip "phase shift" $\sqrt{8m(E-V)} a/\hbar$ differ by 2π . At each such peak the reflections from the barriers at $x=0$ and $x=a$ interfere destructively so that the reflection is zero. In this regime the behavior of the barrier is reminiscent of that of the optical Fabry-Pérot interferometer (etalon).³ This is an optical device that in its simplest embodiment consists of a slab of transparent solid with flat and parallel end faces. The transmission as a function of frequency of light incident on the etalon is described by a function similar to (4.24) and the mathematics involved in treating it is identical to that used in this section.

In conclusion we may note that the case of the inverted barrier, shown as a dashed curve in Fig. 4.5, is obtained by merely replacing V with $-|V|$ in (4.24). The potential well in this case is identical to the one considered in Section 4.2, except that here $E > V$ and, consequently, the solutions for E larger than 0 are unbound (sinusoidal everywhere), while in Section 4.2 we considered bound states only. In the unbound regime the energy E may take on any value. In other words, we can obtain a solution of the Schrödinger equation in the form (4.20) satisfying the boundary conditions for any E . In the bound regime discussed in Section 4.2, only a finite number of discrete eigenvalues E exist. We thus find that the complete spectrum of eigenvalues E of the potential well is part discrete and part continuous.

³M. Born and E. Wolf, *Principles of Optics*, 3rd ed. (Pergamon, New York, 1965), Chapter 7.

*Photons
wavefront
on finite
medium
not suitable
Substituting
show to
complete
wave*

4.4 PHYSICAL MANIFESTATION OF PARTICLE TUNNELING

α Decay of Nuclei

The decay of nuclei by emission of an α particle can be viewed as a tunneling process. The nucleus before a decay event can be thought of as an α particle (a helium nucleus) trapped in a spherical potential well, which represents its interaction with the rest of the nucleus. The potential energy of the α particle as a function of its distance r from the rest of the nuclear mass is sketched in Fig. 4.7. The behavior at large r is due to Coulomb repulsion between the like charges, while at $r < R$ ($R \sim 10^{-15}$ cm) it is dominated by the nuclear forces and is attractive. The particle of energy E less than the maximum in the potential well may be thought of as bouncing between the two sides of the well with a small probability of tunneling through and escaping upon each incidence.

The tunneling probability per unit time (the inverse of the decay lifetime) is equal to the number of bounces per unit time multiplied by the tunneling probability per incidence. The bouncing rate is approximately

$$\omega \sim \frac{v}{R} \approx \frac{p}{mR} \approx \frac{\hbar k}{mR} \approx \frac{\hbar \pi}{mR^2}$$

where v is the velocity of the particle and we used (4.1) to write $k \sim \pi/R$. The

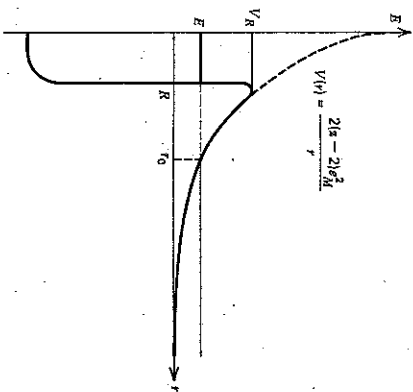


Figure 4.7 Energy diagram of the mutual potential between an α -particle ($z=2$) and "daughter" nucleus whose charge $=(z-2)e$. For large distances ($r \gg 10^{-14}$ m) it is simply the Coulomb repulsion. At short distances it is dominated by the nuclear attraction.

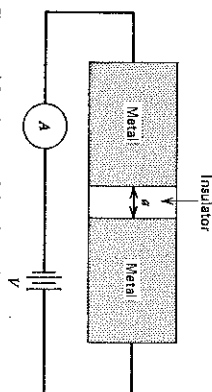


Figure 4.8 A metal-insulator/metal sandwich. When a voltage is applied across the structure, a current flow is established. The electrons cross the insulating material by tunneling.

tunneling probability per incidence is given by (4.26) as

$$T(E) \sim 4 \left(\frac{E}{V} \right) \left(1 - \frac{E}{V} \right) \exp \left(- \frac{\sqrt{8m(V-E)}}{\hbar^2} (r_0 - R) \right)$$

The decay rate is thus determined predominantly by the exponential factor in $T(E)$. Its actual value is very sensitive to the exact shape of the potential curve and can vary by many orders of magnitude from nucleus to nucleus.

Tunneling in Solids

Another manifestation of tunneling occurs in solid state physics. Consider two conductors (Fig. 4.8) (this may include superconductors and semiconductors) that are separated by a thin (~ 10 Å) layer of an insulator. When a voltage is impressed across the "sandwich" a current will be observed to flow. This current is due to electrons crossing from one metal to another by tunneling through the potential barrier presented by the insulator.⁴ The tunneling nature of this current is established by noting its exponential dependence on the insulator thickness a in accordance with (4.26).

For the student of electromagnetic theory we may point out the exact formal similarity of electron tunneling and propagation of electromagnetic modes in waveguides below cutoff.⁵

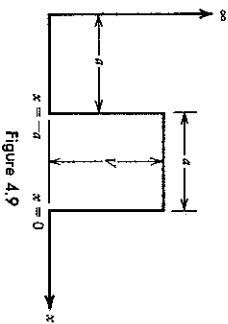
PROBLEMS

1. Obtain the solution $\psi_E(x)$ for a potential well

$$V(x) = \infty \quad (x < 0); \quad V(x) = 0 \quad (0 < x < a); \quad V(x) = V_0 \quad (x > a).$$

⁴This potential barrier is due to the fact that when dissimilar materials are brought into contact their chemical potentials are equalized through electric charge transfer so that potential gradients are set up.

⁵See, for example, S. Ramo, J. R. Whinnery, and T. Van Duzen, *Fields and Waves in Communication Electronics* (John Wiley and Sons, New York, 1960), p. 422.



2. (a) Complete the algebra and derive D in (4.22).
(b) Prove (4.25).

3. Using any convenient references, describe the formal analogy between the evanescent phenomena of electron tunneling and that of propagation of electromagnetic waveguide modes at frequencies below cutoff.
4. Formulate the one-dimensional problem of the transmission and reflection of an incident electron from two potential barriers, each of the form of Fig. 4.5a, which are separated by a distance d .

Hint: It will prove profitable to develop a matrix formalism to describe the effect of any single well on the eigenfunction. The matrix should relate the incident and reflected waves at one plane to those at some other plane.

5. Extend the matrix technique of Problem 4 to describe the propagation of an electron through an arbitrary sequence of rectangular barriers.
6. Estimate the lifetime of a particle of mass m trapped in the potential well shown in Fig. 4.9.

Hint: The system shown does not possess trapped particle eigenstates corresponding to a trapped particle, since such a particle will "leak" away through tunneling. For the purpose of the approximate estimate of the lifetime, we may assume that $V = \infty$ when deriving the eigenfunctions of the trapped particle. The latter may be assumed to be incident on the boundary $x = 0$ with a velocity $v \approx \hbar k/m$ and a frequency v/a .

CHAPTER FIVE

The Harmonic Oscillator

In this chapter we consider the eigenvalue problem of the harmonic oscillator. The idealized harmonic oscillator is taken as a point mass connected to the end of a frictionless idealized spring (i.e., a spring in which the restoring force is proportional to its elongation). A number of very important problems—including the quantum treatment of electromagnetic modes, lattice vibrations—and even the electrical engineer's RLC "tank" circuit—can be modeled as a harmonic oscillator. The study of the harmonic oscillator is thus of fundamental importance in quantum mechanics. The mathematical techniques employed are very elegant and are crucial to consideration of quantum optics, fluctuation theory, noise, and coherence. Obviously, this is one topic we cannot avoid.

5.1 PARITY

Before delving into the problem of the harmonic oscillator we introduce the concept of parity to which we already alluded in Section 4.1. Consider the time-independent Schrödinger equation of a particle moving in a potential field $V(\mathbf{r})$:

$$-\frac{\hbar^2}{2m} \nabla^2 u_{\mathbf{E}}(\mathbf{r}) + V(\mathbf{r})u_{\mathbf{E}}(\mathbf{r}) = E u_{\mathbf{E}}(\mathbf{r}) \quad (5.1)$$

Let the potential function $V(\mathbf{r})$ possess inversion symmetry, that is,

$$V(-\mathbf{r}) = V(\mathbf{r}) \quad (5.2)$$

It follows that

$$-\frac{\hbar^2}{2m} \nabla^2 u_{\mathbf{E}}(-\mathbf{r}) + V(\mathbf{r})u_{\mathbf{E}}(-\mathbf{r}) = E u_{\mathbf{E}}(-\mathbf{r}) \quad (5.3)$$

so that $u_{\mathbf{E}}(-\mathbf{r})$ is an eigenfunction of the same Hamiltonian as $u_{\mathbf{E}}(\mathbf{r})$ with the